Evolution of the NMC Data Assimilation System: September 1978–January 1982

ROBERT E. KISTLER AND DAVID F. PARRISH

National Meteorological Center, NWS, NOAA, Washington, DC 20233

(Manuscript received 22 March 1982, in final form 16 June 1982)

ABSTRACT

The evolution of the NMC global data assimilation system in the period 1978–81 is presented. The improvements include revisions to the analysis programs and the replacement of the initialization and the prediction model. Data are analyzed over a finer analysis grid, are scrutinized by a more thorough "buddy check," and are subject to a multivariate wind relationship. The impact of the changes upon the wind analysis is examined with respect to the case of 1200 GMT, 21 October 1979. The system changes concurrent with the addition of the spectral prediction model are noted. Experimental evidence demonstrates the superiority of the spectral system with respect to the gridpoint system previously in use.

1. Introduction

As the record of automated, global analyses of the atmosphere continues to accumulate, interest in the incorporation of these daily analyses into climatic analyses has grown as well. Through the auspices of the National Center for Atmospheric Research (NCAR), researchers have access to National Meteorological Center (NMC) global analyses produced daily for 0000 and 1200 GMT. Currently, two analyses are available for each analysis time, differing by data cut-off and analysis method, yet having a common background or "guess" field. The analysis with the earlier data cut-off of ~3.5 h is the Hough analysis of Flattery (1971). The later, "final" analysis, with about a 9.5 h cut-off, is the optimum interpolation (OI) analysis of Bergman (1979). The OI analysis is an integral part of the NMC global data assimilation system (GDAS) as described by McPherson *et al.* (1979). The GDAS, in the process of its 6 hr analysis/forecast cycle, provides the common guess field used by both analysis systems.

In the concluding remarks of McPherson *et al.* (1979), the evolutionary nature of the GDAS was expressed, ". . . the system will prove to be an evolutionary one, undergoing modification as improvements are developed and tested." Unfortunately, such modifications might occasionally lead to misinterpretations when the operational analyses are used in a climatic investigation. In light of this possibility, the purpose of this note is to inform current and future users of the NMC global analyses of changes to the NMC GDAS for the period September 1978–January 1982.

The GDAS may be viewed as a three-component system—an analysis, an initialization, and a prediction model. In the interim since the implementation on 22 September 1978 of the GDAS described by McPherson *et al.* (1979), revisions to all three components have taken place. Section 2 of this note discusses an alteration of the analysis grid arrangement and modifications to the quality control of data. Section 3 reports on the experimentation that preceded the replacement of the initialization and prediction model. Section 4 outlines a revision to the multivariate structure of the OI analysis that was prompted by the new initialization. The paper concludes with a summary.

2. Analysis changes in response to FGGE data

a. New analysis grid

On 11 October 1979, the first significant revisions occurred to the GDAS described by McPherson *et al.* (1979). One of the two changes involved replacing the 5 × 5° latitude–longitude grid with one more suitable for objective analysis—a 3.75° modified Kurihara (1965) type grid. By avoiding the redundant longitudinal grid spacing near the poles of the latitude–longitude grid, the new analysis grid permits an increased resolution in the Tropics at the minimal cost of increasing the total number of grid points by 10%.

Concurrent with the new analysis grid came a reduction in the number of observations permitted to influence an analysis point. The maximum was reduced from 10 to 8. A limited sample of parallel experiments was run to assess the impact of the two changes. The results (not shown) indicated that the revised analysis tended to more closely fit the data than its predecessor. The reduction in permitted observations was motivated by the additional computational time that would result from the introduction

of the NOAA-6 satellite temperature soundings to the GDAS data base. Because only a week separated the implementation of the analysis changes and the introduction of the NOAA-6 data, any unique influences that could be attributed to the new analysis were likely obscured.

b. *Buddy check*

In an article addressing the error levels of data, Bergman (1978) outlined the multi-level quality control approach that was originally incorporated in the present system. Subsequently, two revisions have been made.

The first involves a refinement to the inter-observational, consistency check, i.e., "the buddy check." Whereas the original formulation sought only to exclude data, the revised scheme works both ways. Previously, a single set of flags was tabulated (c.f. Bergman, 1978, Table 2) whenever the difference of two residuals (observation − guess) exceeded a limit inversely proportional to the interdata correlation. In the revised system an additional tabulation counts the number of residual pairs whose differences do not exceed the allowable tolerance, i.e., they corroborate each other. A residual is kept if its corroboration count equals or exceeds two. The method fails only when three or more erroneous residuals are mutually consistent.

This revised buddy check is particularly helpful to the surface pressure analysis in areas of rapid cyclogenesis. The prediction model usually locates these storms fairly accurately but tends to underestimate the central pressure. The previous system often excluded observations defining the central pressure because their large residuals were judged inconsistent with those well-removed from the center. The new system makes it possible for the central residuals to be corroborated by nearer neighbors and not excluded by peripheral data.

The second change in quality control procedures avoids the possible inconsistent data screening that had existed previously. The former system intercompared only the ten or fewer residuals selected for the update at a particular location at the time when the update was about to be performed.[1] Consequently, it often led to the undesirable circumstance of a particular observation being kept at one point and excluded at another. This situation has been alleviated by performing all data screening in a separate step prior to analysis.

In this step, the buddy check outlined above is performed using every other analysis grid point at points of reference (Fig. 1). The data screening assumes a univariate two-dimensional analysis, and is applied to the 12 mandatory levels from 1000 to 50 mb. Off-level data are assumed valid at the next higher standard level. When mass data are to be screened, a circular area, as depicted in Fig. 1, outlines the area of data to be screened. Data between the circle and outer square are not judged themselves but may influence the decision to keep or toss data within the circle. The areal extent of the circle is sufficiently large so as to insure that each observation is screened at least once as the checking process sequences over the globe.

In the case of wind observations the u- and v-components are screened independently. Since the correlation functions for the wind components are not isotropic (see Bergman, 1979, Fig. 1), the data within the square area are screened. The application of these two improvements halved the number of reports which were excluded in the earlier system. The revised buddy check was implemented in the summer of 1980.

3. A new prediction model

Since the inception of the NMC GDAS, the prediction model component has been the nine-layer global gridpoint model (Stackpole, 1978), hereafter noted as 9L. Unfortunately, throughout its period of service, 9L has been characterized by a disturbing level of noise. While several promising solutions have been proposed, each created side effects as troublesome as the noise itself (e.g., Dey, 1978).

In sharp contrast to the noisy character of 9L is the noise-free behavior offered by the combination of a nonlinear, normal-mode initialization (NLNMI), and the NMC spectral model (Sela, 1980). The NLNMI follows the design of Machenhauer (1977) and has been implemented with the spectral model by Ballish (1981). It employs the conventional two iterations and, in the experiment to be described, adjusts the gravest six vertical modes.

a. *Intercomparison of the models*

To replace the 9L with the spectral model it was necessary to demonstrate its superiority in a parallel test. Before describing that experiment it is appropriate to contrast the two systems. The salient features of each are summarized in Table 1. The notable differences include differing time integration methods, radiation modeling, time and space filtering, and vertical discretization. The incorporation of large-scale precipitation processes was common to both models. The algorithms developed for the 9L have been included without modification in the spectral model. Moist convection in the spectral model has been adapted from the nested grid model of Phillips (1979).

The version of the spectral model tested did not contain radiation parameterization. In the absence

[1] The surface pressure analysis continues to use a maximum of 10 observations, although the maximum in the upper air analysis has been reduced to 8.

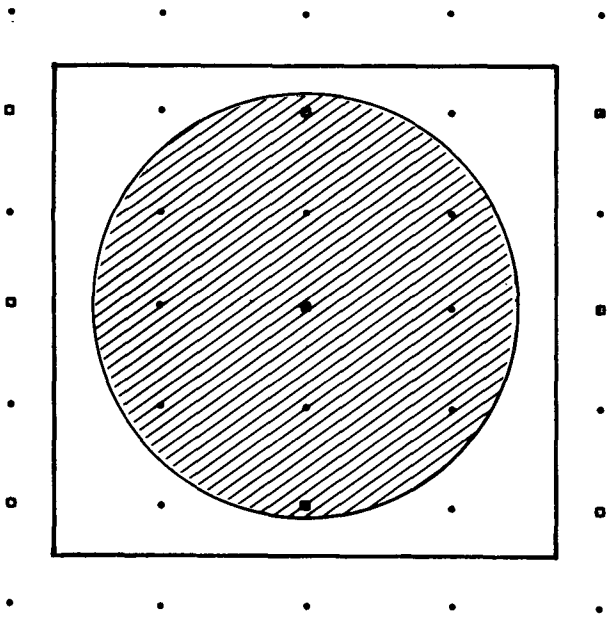

FIG. 1. Relationship of analysis grid (points), buddy check grid (squares), area of data to be screened (circle) and area of data influencing the screening (square).

of radiative heating and cooling, the thermal structure of the atmosphere would have to be specified by data, the majority of which was provided by two polar orbiting satellites. It was recognized that satellite temperature retrievals have shortcomings, e.g., lack of variances (Tracton *et al.*, 1980). However, all preliminary evidence indicated that the replacement of the incumbent 9L by the spectral model would alleviate numerical problems that overshadowed the question of whether the satellite data adequately describes the atmospheric thermal structure. Nevertheless, it is imperative that the tuned radiative package be included at the earliest possible date.

Of the differences noted in Table 1, the details of the two vertical coordinates merit closer examination. The sigma structures in each model are compared in Fig. 2. The atmosphere in 9L is divided into two sigma domains separated by a tropopause, which acts as a material surface. The model is capped at 50 mb. The tropospheric domain contains six equally spaced layers, while the stratospheric domain has three equally spaced layers.

The spectral system contains a single sigma domain between the surface and 0 mb, subdivided into 12 layers of varying pressure thickness. Structure A represents the arrangement used in the tests described in the following section. Structure B is the spacing that is currently in use.

b. Parallel experiment

In recommending that the spectral system replace the 9L in daily operations, a formal test comparing the performance of the systems was required, anal-

TABLE 1. Summary of attributes of the competing systems.*

Attribute	9L	Spectral
Vertical resolution	9L (6L moist)	12L (6L moist)
Tropopause	Material surface	None
Representation of model variables	Gridpoint	Spectral
Horizontal resolution prediction model	2.5° × 2.5° lat–long	24 waves rhomboidal
Top of model	50 mb	0 mb
Radiation	Yes	No
Latent heat release	Yes	Yes
Initialization	Dey (dynamic)	Machenhauer NLNMI
Filtering:		
Time	Strong	Weak
Horizontal	None	$K \cdot \nabla^4$ operator
Time integration	Leapfrog	Semi-implicit centered
Analysis	OI	OI
Horizontal resolution	UA ~ 3.75° modified Kurihara	UA ~ 3 × 4° modified Kurihara on gaussian latitudes
	SFC 2.5° × 2.5° lat–long	SFC 2.5° × 2.5° lat–long
Smoothing of fields	Spectral filtering: 35 waves troposphere 24 waves stratosphere (triangular truncation)	None

* UA = upper air, SFC = surface pressure.

ogous to the 5½-day test described by McPherson *et al.* (1979). In this instance, a seven-day period, 0000 GMT, 12 December 1979 through 0000 GMT, 19 December 1979 was chosen. Each system was judged on the accuracy of the analyses and of the predictions made from within the 6-h analysis–forecast cycle valid at each of the synoptic times of 0000 and 1200 GMT throughout the seven-day period. Root-mean-square (rms) and bias differences between selected radiosonde observations and the analysis and prediction for each synoptic time were tabulated at four mandatory pressure levels: 850, 500, 250 and 100 mb. For each pressure level, the rms and bias differences were calculated for the heights, temperatures, wind speed, vector wind error and relative humidity (850 and 500 mb only). The selected rawinsondes were arranged into six networks:

Northern Hemisphere	102 stations (NH102)
North America	110 stations (NA110)
Europe	96 stations (EUR96)
Southern North Atlantic	42 stations (SNATL42)
Southern North Pacific	48 stations (SNPAC48)
Southern Hemisphere	31 stations (SH31)

The rms and bias scores for the 14 verification times were then averaged by variable, level and network. Hereafter, all references to rms and bias scores will be the scores averaged over the seven-day period.

Table 2 presents a tabulation of which system produced the lower rms score, summarized by network, level and variable for both the predictions and analyses. Unequivocally, the spectral system outscores the 9L system in all of the broader summaries. Only when the scores are differentiated by level and variable does the 9L system win one of the 18 possible comparisons—that for 100 mb temperature. Insight into this curious anomaly is gained from viewing profiles of temperature, rms and bias scores in Fig. 3. Since the behavior of the predictions and analyses in this regard are similar, only the profiles of the prediction are shown. The upper and lower halves of the figure show profiles for extratropical and tropical data networks, respectively. The 100 mb error for the spectral model is dominated by a large bias in the profiles in the lower half, in marked contrast to the extratropical profiles of the upper half. The cause of this behavior is rooted in the vertical coordinates of the two systems; primarily, it is due to the absence of an explicit tropopause in the spectral system. As depicted in Fig. 2, when the tropopause is located near 100 mb, as it would tend to be over the tropical networks summarized in the lower half of Fig. 3, the resolution of the stratospheric domain in the 9L system can better define the temperature profile discontinuity at the tropopause. However, when the level of the tropopause lowers to 217 mb or greater, the spectral resolution becomes equal to or better than that of the 9L. Furthermore, the 9L system has another advantage. The vertical interpolation from sigma coordinates to mandatory pressure levels is not permitted to cross the tropopause; any discontinuity is resolved by a pressure-weighted average of extrapolated temperatures from above and below.

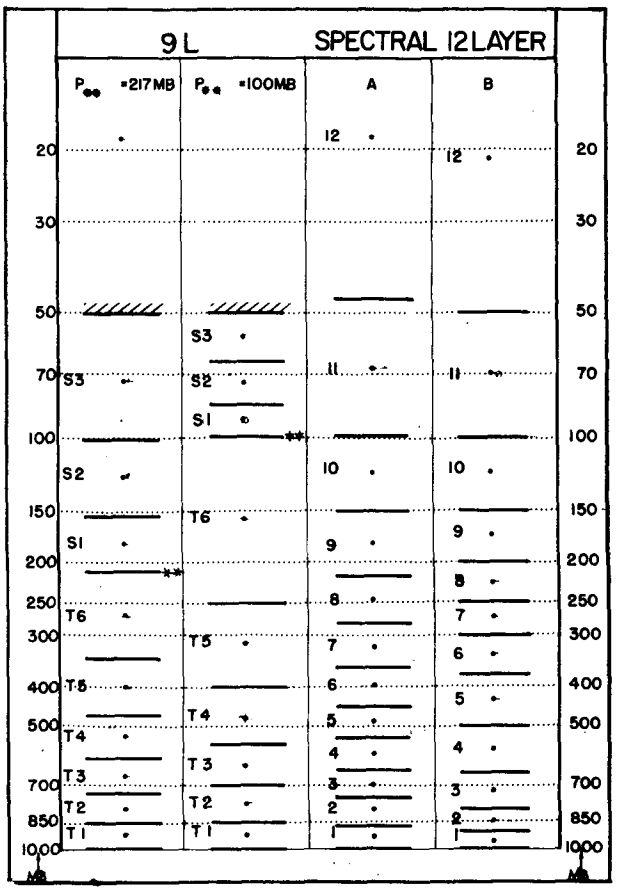

FIG. 2. Comparison of vertical discretization for the 9L gridpoint model and the 12L spectral model. For the 9L model, two examples, differing by tropopause pressure P_{**}, are shown. For the spectral 12L model, column A represents the structure used in the experiment described in the text, while B is the structure in operational use.

While the 9L system performs quite well in handling temperature profiles in high tropopause situations, this advantage is offset by a degradation in resolution in the layers beneath the tropopause. This becomes quite evident when the profiles of forecast wind bias are examined in Fig. 4. In those networks where the spectral model exhibits problems with the temperature bias, the 9L produces the larger bias at 250 mb, a level important to aircraft traffic. While the spectral system suffers from a warm temperature bias, it displays a marked improvement in its wind forecasts compared to 9L. One could expect this type of improvement to feed into the aviation products produced by the NMC large-scale prediction system, for which the GDAS provides the initial guess to its analysis.

In comparison with other system impact tests con-

TABLE 2. Tabulation of lower rms scores for each system. Scores are the averages of the 14 verification times. Four summaries are presented: (a) all levels, all variables, by area: (b) overall; (c) all areas, by level, by variable; (d) all areas, all levels, by variable.

	Method of summary	Area	Predictions			Analyses		
			Spectral	Tie	9L	Spectral	Tie	9L
(a)	All levels, all variables, by area	NH102	14	1	3	7	3	8
		NA110	12	2	4	11	4	3
		EUR96	15	2	1	13	3	2
		SNATL48	14	1	3	9	2	7
		SNPAC42	15	2	1	9	3	6
		SH31	15	0	3	12	1	5
(b)	Overall		85	8	15	61	16	31

			100 mb			250 mb			100 mb			250 mb		
			Spectral	Tie	9L	Spectral	Tie	9L	Spectral	tie	9L	Spectral	Tie	9L
(c)	All areas, by level, by variable	Z	5	0	1	6	0	0	5	0	1	6	0	0
		T	1	0	5	5	1	0	1	0	5	5	1	0
		RH	—	—	—	—	—	—	—	—	—	—	—	—
		|V|	4	1	1	5	1	0	4	1	1	5	1	0
		V	5	1	1	4	0	2	5	1	1	4	0	2
			500 mb			850 mb			500 mb			850 mb		
		Z	6	0	0	5	0	1	6	0	0	5	0	1
		T	5	0	1	2	2	2	5	0	1	2	2	2
		RH	6	0	0	4	0	2	6	0	0	4	0	2
		|V|	4	0	2	5	1	0	4	0	2	5	1	0
		V	5	0	1	6	0	0	5	0	1	5	0	0
(d)	By variable, all areas, all levels	Z	22	0	2				18	2	4			
		T	13	3	8				10	4	10			
		RH	10	0	2				8	0	4			
		|V|	18	3	3				10	6	8			
		V	20	1	3				15	4	5			

ducted recently at NMC (e.g., Tracton *et al.*, 1980), the results of this study are overwhelmingly conclusive. The spectral system could be implemented with the expectation that the overall accuracy of the analyses and predictions of the GDAS would be improved.

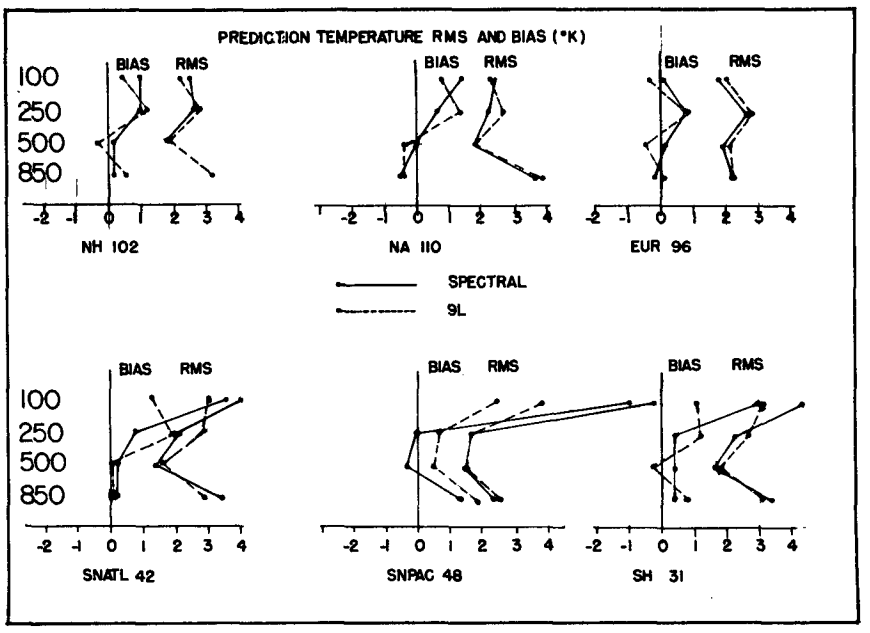

FIG. 3. Forecast temperature (°C) bias and rms profiles for each network area.

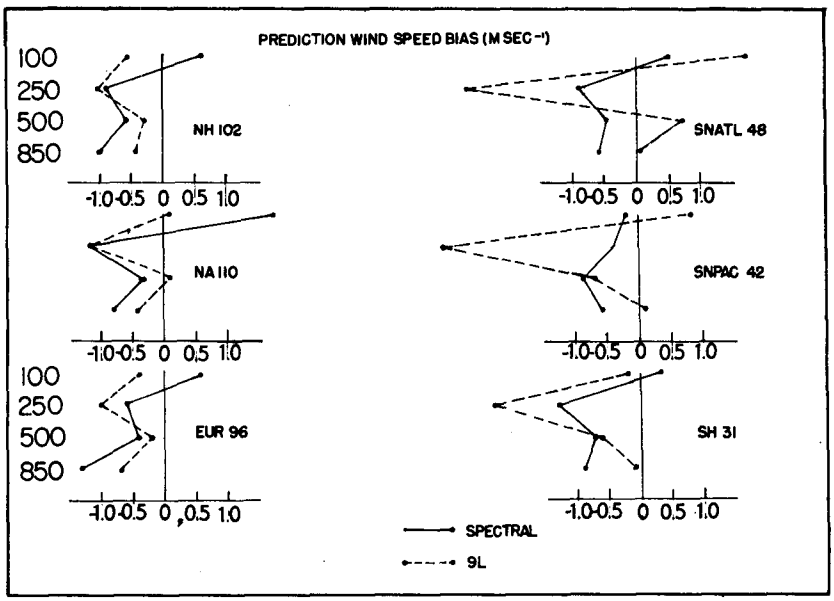

FIG. 4. Forecast wind speed (m s^{-1}) bias and rms profiles for each network area.

4. The case of 1200 GMT, 21 October 1979, and the mass–motion balance

While introduction of the spectral system would help overcome the persistent noise problem of the 9L system, another basic problem of data assimilation resurfaced, namely, that of data rejection. Attention was drawn to this problem by the circumstances involving analyses in the Gulf of Alaska at 1200 GMT, 21 October 1979. A discussion of the synoptic situation was given by Phillips (1980) in which he raised two interrelated questions:

1) If the satellite data had been received on time for the NMC analyses, could the large errors in the subsequent predictions have been avoided?

2) More fundamentally, could the wind analysis be suitably adjusted to reflect the intense circulation implied by the observed mass field?

The case had drawn attention because, at first appearance, an erroneous forecast over the central United States was assumed to be related to a lack of satellite data over the eastern Pacific two days earlier. This case was chosen not only to answer question 1), but to also serve as an opportunity to evaluate the performance of the then recently constructed GDAS based upon the NMC spectral model.

It was decided to run a satellite data impact test on the case using the spectral assimilation system, which was still experimental at the time. Two parallel assimilations were run over the period 0000–1200 GMT, 21 October: one including the satellite data, one excluding it. From each 1200 GMT analysis, a 48-hour prediction was run. Curiously, objective and subjective evaluation of the two forecasts had scores virtually identical to those of the original, erroneous forecast. Considering the magnitude of the differences between the satellite data and the analysis prepared without it, some mechanism was obviously purging the effect of the data prior to the prediction. That mechanism proved to be the NLNMI. As Daley and Puri (1980) so graphically demonstrated, unless the wind field is correspondingly adjusted to the observed mass field, a NLNMI will simply reject the mass information in favor of the original wind field. Accordingly, Phillips' second question was raised. Rephrasing the question bluntly, why had the multivariate aspect of the OI analysis not adjusted the winds sufficiently to avoid the data rejection by the initialization?

The fundamental problem was outlined by a caveat in Bergman (1979): "The data selection procedure is the most arbitrary aspect of the entire analysis method, and is in need of improvement provided such improvement can be made without appreciably increasing machine time." To be specific, each observation within approximately 1500 miles of the analysis point is screened for possible selection. Computational restrictions limit the number of observations; the current operational environment will permit a maximum of eight. The decision as to whether or not an observation is included in the analysis is determined by the magnitude of the modeled correlation for the type of data and the variable being analyzed. (See Bergman, 1979, Figs. 1 and 2 for the respective horizontal and vertical correlation functions.) First, data with the magnitude of the correlation less than 0.1 are discarded. Then the remaining data are ordered according to the magnitude of the correlations, with the eight largest values being se-

TABLE 3. Effect of mass data selection on a wind update.

Pressure (mb)	Residuals		Weights			
	t (°C)	Z (m)	t_{450}, t_{350}	all t	all Z	Z_{400}
85	−1.9		—	+0.9		
100		+4.4	—		0.0	
125	−1.1		—	+0.14		
150		+15.8	—		0.0	
175	−0.2		—	+0.16		
200		+17.7	—		−0.02	
225	+0.2		—	+0.14		
250		+16.5	—		+0.05	
275	+0.5		—	+0.17		
300		+14.0			−0.05	
350	+1.0		+0.18	+0.20		
400		+5.9			−0.49	−0.53
450	+1.4		−0.19	−0.13		
500		−2.9	—		−0.03	
600	+1.3		—	−0.15		
700		−14.3	—		+0.02	
777	−0.1		—	−0.07		
850		−13.9	—		−0.02	
928	−0.09		—	−0.08		
1000		−9.9	—		+0.01	
		u_{400} correction:	−0.07	−0.43	−0.43	−0.43

lected. The fallacy of these restrictions—only 8 observations, a minimum correlation of 0.1—in terms of its impact upon the mass–motion balance is demonstrated by an example adapted from McPherson (1980).

The preferable situation, setting aside computational restrictions, would be to permit all the data that are correlated with the analysis point to influence the analysis. However, a demonstration of how these arbitrary restrictions hamper the mass motion balance does not require examination of an OI analysis incorporating several soundings. A simpler example will suffice, one in which only one temperature sounding influences a wind component at a given pressure level.

Assume that the u component of the wind is to be updated at 400 mb by a profile of mass data located 750 km to the north (i.e., a maximum of correlation). A sample profile of thickness temperature residuals is given in the second column of Table 3. When the data selection procedure is restricted to include only observations with an absolute value of correlation of 0.1, only two of the 12 available levels are selected. When the error minimization problem is solved, the weights for these two levels (column 4) nearly cancel each other. However, simply removing the threshold restriction from the selection procedure allows the entire profile into the problem, and the magnitude of the wind correction is increased over six fold. Unfortunately, this approach to the multivariate analysis would result in a prohibitively large increase in computation time.

However, a workable alternative was available. The original formulation of the multivariate aspect of the analysis was based upon the thermal wind relationship. That relationship may be viewed as the combination of the hydrostatic assumption in the vertical and the geostrophic assumption in the horizontal. The latter assumption may serve as the basis for the multivariate approach; see, e.g., Schlatter (1975). In that approach, the height–height autocorrelation, z–z, serves as the basis for the z–u and z–v cross-correlations. Furthermore, the z–z correlation may serve as a basis to calculate the vertical correlations between heights and temperatures, z–t and t–z, using the hydrostatic relationship.

In the third column of Table 3 are the height residuals that were calculated by performing an analysis using the z–t cross-correlations and the temperature residuals as data. These height residuals were then applied to the analysis problem of updating the wind correction at 400 mb. The sixth column depicts the weights derived when the entire profile of heights was applied. Note that the calculated correction, −0.43 m s^{-1}, corresponds exactly to the result when the entire profile of temperature residuals was used, as would be expected. However, the desired combination of accuracy without additional computational cost resulted when just the height residual at 400 mb was made available to the analysis. The result in this instance is noted in the seventh column of the table by a weight of −0.49 along with a repeat of the −0.43 m s^{-1} wind correction.

This example demonstrated that the wind analysis

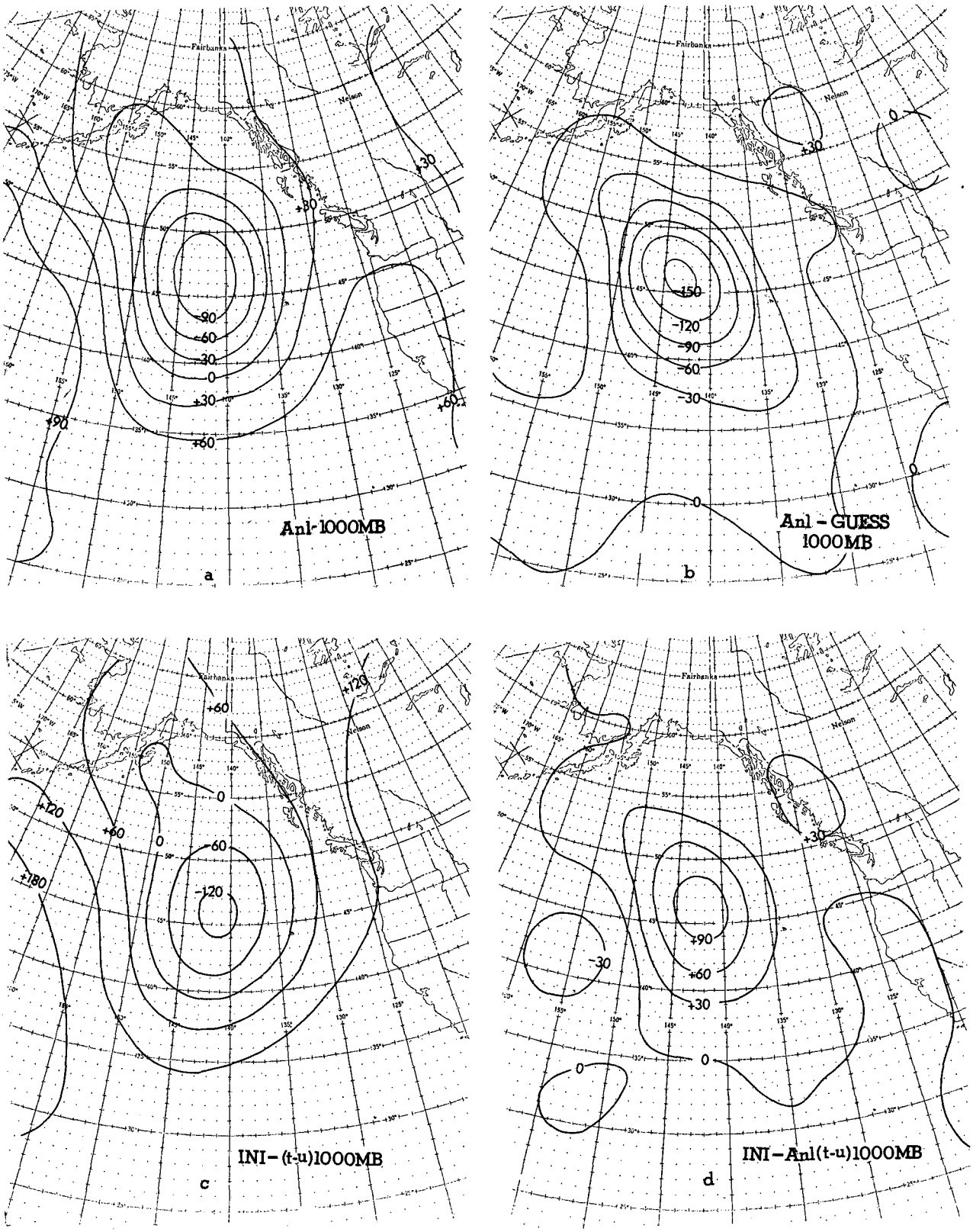

FIG. 5. 1000 mb height and height differences fields: (a) OI analysis (ANL); (b) the correction field (ANL-GUESS); (c) field following NLNMI (INI) where the winds were analyzed with a t–u correlation function; (d) rejection field from t–u correlation wind analysis (INI-ANL); (e), (f) as in (c), (d) except that z–u correlation was used in the wind analysis.

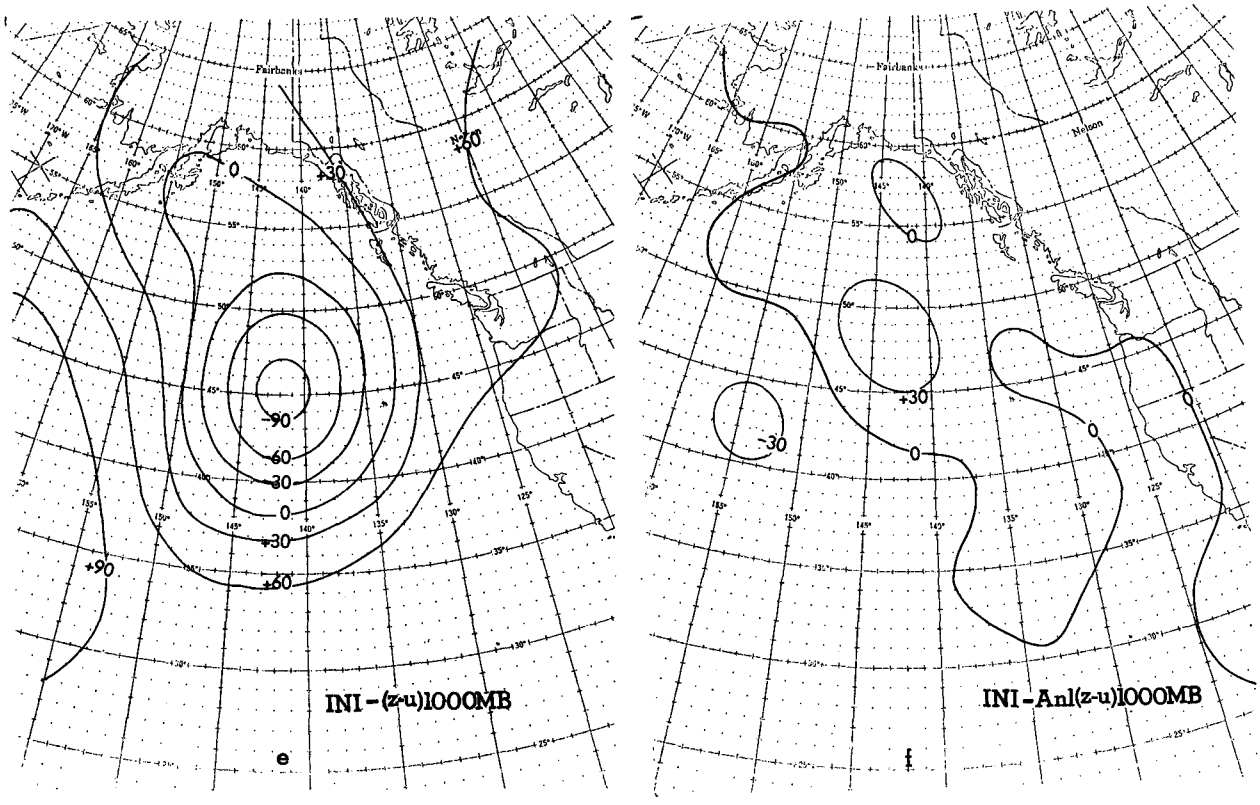

FIG. 5. (*Continued*)

had been handicapped by the data selection procedure. It could function as originally designed, without additional computation cost, if height (rather than temperature) residuals were selected and analyzed via z–u and z–v correlations.[2]

It was a simple change to include height residuals because the raw mass inputs to the analysis are the mandatory level height observations. Thickness temperatures are calculated from the predicted and observed heights and then are differenced to form the residuals. In the revised procedure, residuals for both heights and temperatures are calculated, stored, and passed to the analysis. One minor compromise for computational efficiency was made. Instead of calculating height residuals from the temperature residuals via a single column analysis, as was noted in the results of Table 2, the height residuals are calculated directly during the process of calculating the thickness temperature residuals.

The impact of the z–u correlation in the wind analysis is evident in Figs. 5 and 6. These figures depict the 1000- and 500-mb height contours for the analysis (ANL) and the initialization (INI) for each method. In addition, difference charts of the correction field (ANL-GUESS) and the rejection field (INI-ANL) are also displayed. The Analysis (ANL), panel (a) and the corrections field (ANL-GUESS), panel (b), apply to each method of wind correlation since the accompanying mass field analyses were performed identically. The importance of the z–u approach is seen in the comparison of the INI-ANL fields. Note, for the t–u correlation in Figs. 5 and 6, panels (c) and (d), that the rejection amounts to half the correction at 1000 mb and nearly two thirds of that at 500 mb. However, substitution of the z–u procedure, panels e and f, substantially reduces the degree of rejection. Panel (f) in Figs. 5 and 6 indicates rejection values half the size of the corresponding values in panel (d).

In response to Phillips' question as to whether the winds of the analysis could be modified to reflect the satellite temperatures, the answer is yes. In addressing the first question, whether the inclusion of satellite temperature data would improve the prediction, in this instance a forecast produced with the modified winds made little difference. This system in the Pacific simply did not interact strongly with the developing storm system over the United States. Nevertheless, this case helped formulate an improvement to the GDAS such that in cases where satellite data may make a difference, their presence has a greater chance of having a positive influence.

[2] Subsequent examinations have revealed that the mass/motion balance can be further improved by selecting the *same* set of residuals for both mass and motion analyses.

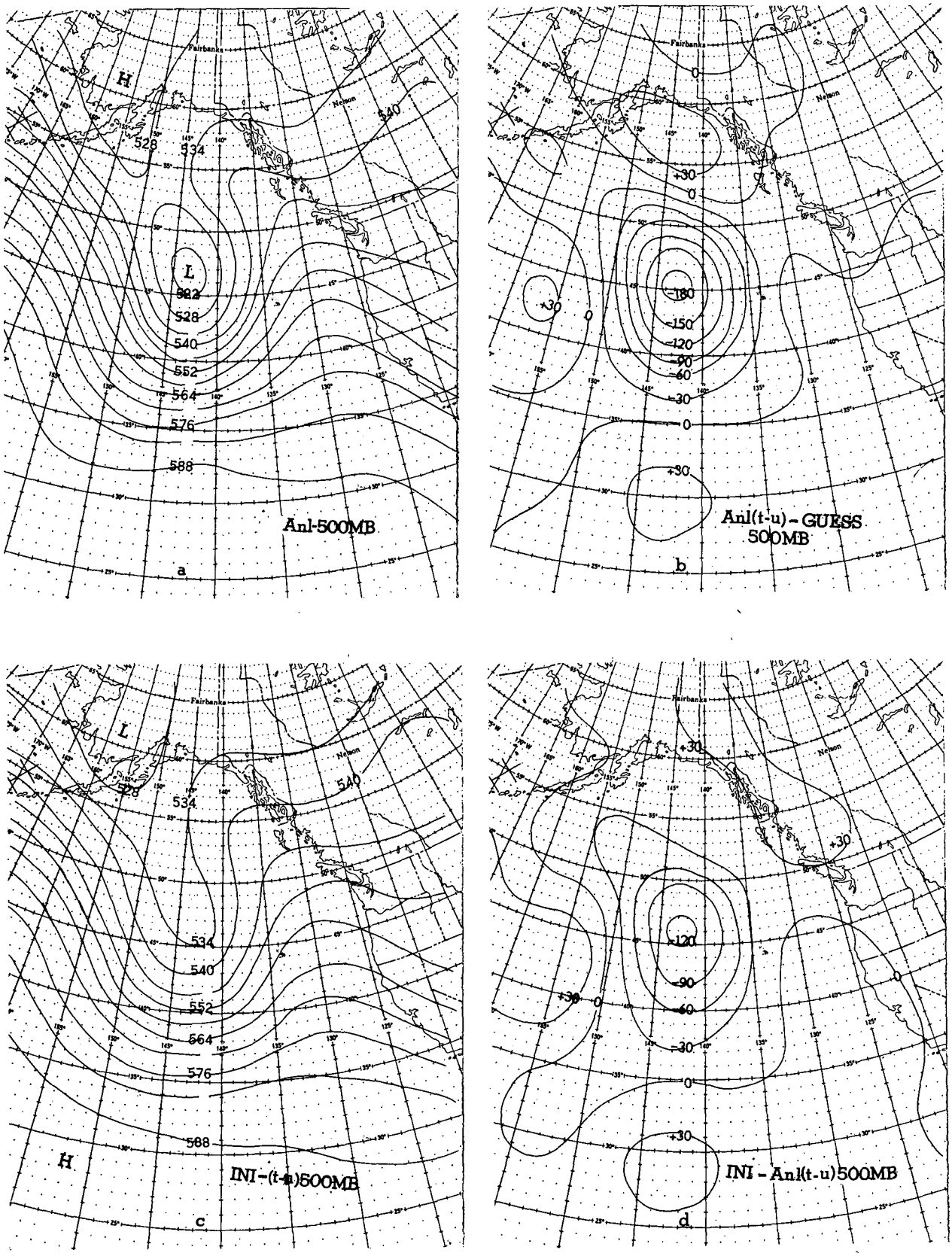

FIG. 6. As in Fig. 5, but for 500 mb height and height difference fields.

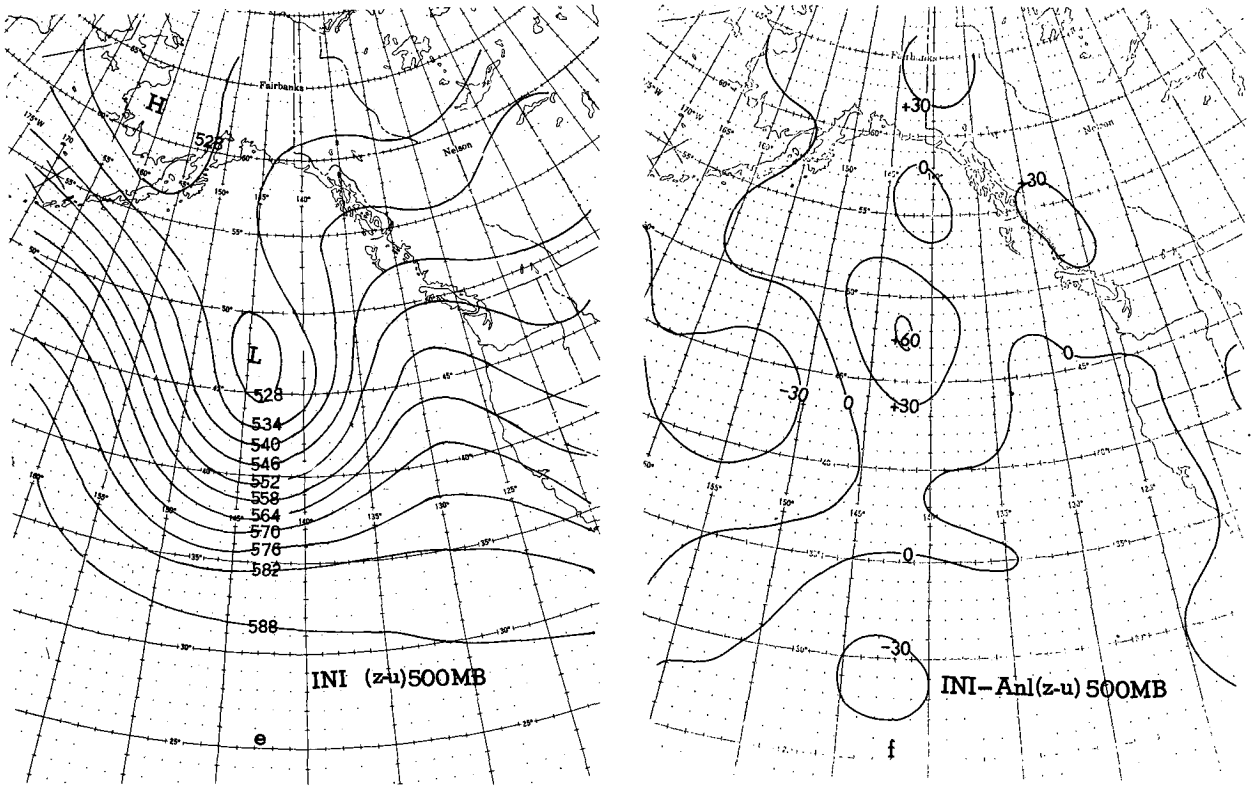

FIG. 6. (*Continued*)

We have only looked at the problem of updating winds with temperature data. The deficiencies of the data selection process might also adversely affect the multivariate update of the thickness temperature with wind data. Although the wind analysis was strengthened by the conversion to the $z-u$ correlation, as simple an alternative was not available to the thickness temperature analysis. Furthermore, the barotropic experiments of Daley and Puri (1980) and the experimental evidence just presented indicated that the predominant scale of the correction fields is such that the mass fields are adjusted to the winds. Consequently, it was decided to analyze the thickness temperatures univariately, resolve the imbalances with the winds fields via the NLNMI, and archive the results as the analysis of record. Therefore, beginning on 27 May 1980 the NMC "final" analyses (9.5 h data cutoff) reflect 1) guess fields provided by the spectral model, 2) a univariate mass analysis and a $z-u$ correlation, multivariate wind analysis, and 3) adjustments imposed by the NLNMI.

A few remarks regarding the adjustment imposed by the NLNMI are appropriate. Although the NLNMI played an important role in enabling the spectral system to outperform the 9L, it has posed several problems itself. While it effectively suppressed gravity wave noise, the NLNMI also acts indiscriminately, causing underestimates of organized vertical motions in the tropics (e.g. the Hadley circulation). Confronted with the choice of deciding at which point to archive the results of the analysis, we chose to do so following the NLNMI, thereby trading-off the weakened tropical circulation in favor of noise-free extratropical circulations.

The GDAS remained in the configuration just described until 13 January 1982 when a "pseudo-wind" analysis approach was implemented. In that approach, gradient winds computed from the univariate mass analysis are provided to the wind analysis as "pseudo-observations." A description of this method and other modifications currently underway will be forthcoming.

5. Summary

The NMC global data assimilation system has continued to evolve from the status reported by McPherson *et al.* (1979). Improvements implemented in the period 1978–81 are noted. Included among these are several changes made to the optimum interpolation analysis program to improve its accuracy. The analysis grid is now an equal area arrangement with a finer latitudinal spacing than the previous grid. The buddy check of data has been upgraded to screen

the data more carefully. The multivariate aspect of OI analysis of winds has been strengthened through the adoption of a height–wind correlation function.

The nine-layer model and initialization have been replaced by a 12-layer spectral model and a nonlinear normal mode initialization, respectively. Results from a seven-day parallel experiment clearly demonstrated the superiority of the spectral system. The marked improvement may be attributed to the ability of the spectral system to eliminate noise from the assimilation system.

Acknowledgments. The authors wish to acknowledge the helpful suggestions provided by Drs. Joseph Gerrity and Ronald McPherson. We would also like to thank the referees for their careful reviews. The manuscript was capably typed by Joyce Peters and the graphics carefully drafted by Chuck Burley.

REFERENCES

Ballish, B., 1981: Initialization, theory and application to the NMC spectral model. Ph.D. dissertation, University of Maryland, 151 pp.

Bergman, K., 1978: Role of observational errors in optimum interpolation analysis. *Bull. Amer. Meteor. Soc.*, **59,** 1603–1611.

——, 1979: A multivariate optimum interpolation analysis system of temperature and wind fields. *Mon. Wea. Rev.*, **107,** 1423–1444.

Daley, R., and K. Puri, 1980: Four-dimensional data assimilation and the slow manifold. *Mon. Wea. Rev.*, **108,** 85–99.

Dey, C., 1978: Noise suppression in a primitive equation model. *Mon. Wea. Rev.*, **106,** 159–173.

Flattery, T., 1971: Spectral models for global analysis and forecasting. *Proc. Sixth AWS Technical Exchange Conf.*, U.S. Naval Academy, Annapolis, September, 1970, Air Weather Service Tech. Rep. 242, 42–54 [NTIS AD-724093].

Kurihara, Y., 1965: Numerical integration of the primitive equations on a spherical grid. *Mon. Wea. Rev.*, **93,** 399–415.

Machenhauer, B., 1977: On the dynamics of gravity oscillations in a shallow water model, with applications to non-linear normal mode initialization. *Beitr. Phys. Atmos.*, **50,** 253–271.

McPherson, R. D., K. H. Bergman, R. E. Kistler, G. E. Rasch and D. S. Gordon, 1979: The NMC operational global data assimilation system. *Mon. Wea. Rev.*, **107,** 1445–1461.

——, 1980: Lectures on operational analysis and assimilation of meteorological data. II. Theory of optimum interpolation. NMC Office Note 217, 33 pp. [Available from NMC, 5200 Auth Road, Washington, DC 20233].

Phillips, N. A., 1979: The nested grid model. NOAA Tech. Rep. NWS-22, 79 pp. [Available from NMC, 5200 Auth Road, Washington, DC 20233].

——, 1980: Two examples of satellite temperature retrievals in the North Pacific. *Bull. Amer. Meteor. Soc.*, **61,** 712–717.

Schlatter, T. W., 1975: Some experiments with a multivariate statistical objective analysis scheme. *Mon. Wea. Rev.*, **103,** 246–257.

Sela, J. G., 1980: Spectral modeling at the National Meteorological Center. *Mon. Wea. Rev.*, **108,** 1279–1292.

Stackpole, J., 1978: The NMC 9-layer global primitive equation model on a latitude-longitude grid. NMC Office Note No. 178, 31 pp. [Available from NMC, 5200 Auth Road, Washington, DC 20233].

Tracton, M. S., A. J. Desmarais, R. J. van Haaren and R. D. McPherson, 1980: The impact of satellite soundings on the National Meteorological Center's analysis and forecast system—the Data Systems Test results. *Mon. Wea. Rev.*, **108,** 543–586.